ELSEVIER

Journal of Structural Geology 26 (2004) 419–433

JOURNAL OF STRUCTURAL GEOLOGY

www.elsevier.com/locate/jsg

Successive episodes of normal faulting and fracturing resulting from progressive extension during the uplift of the Holy Cross Mountains, Poland

Andrzej Konon*

Faculty of Geology, University of Warsaw, Al. Żwirki i Wigury 93, 02-089 Warsaw, Poland

Received 20 January 2003

Abstract

Conjugate normal faults, extension fractures and mesh-fracture structures were investigated in Devonian carbonate rocks from the southern part of the Holy Cross Mountains (HCM) (Central Poland). Strata folded during Variscan deformations were later subject to uplift, resulting in increasing extension in the upper part of the rock mass. At a relatively shallow depth, faults and fractures developed in an orderly vertical succession. First, mesh fracture structures and conjugate normal fault sets enclosing acute dihedral angles (2Θ) of over 45° were formed. Next, conjugate normal faults with 2Θ less than 45° and sub-vertical extension fractures developed. The occurrences of conjugate normal sets enclosing different dihedral acute angles and extension fractures with similar strikes, juxtaposed with each other at the same stratigraphic level, point to the fact that the uplifted rock mass underwent successive changes in a stress regime leading to the formation of these structures. The first sets of conjugate normal faults and fractures developed when the HCM were uplifted during a late stage of Variscan deformations. The next sets of extension fractures and conjugate normal faults developed during the following uplift events interrupted by periods of sedimentation of the Mesozoic and younger strata.

Keywords: Normal faults/fractures sets; Successive faults/fractures development; Uplift

1. Introduction

Conjugate normal fault sets and extension fractures are common in areas that have undergone uplift-related extension, developing in response to collision and post-collision shortening in neighbouring mountain belts (e.g. Hancock and Bevan, 1987; Doglioni, 1995). In the post-collisional phase of deformation in the fold belts, uplift commonly occurs (e.g. Mastella, 1988; Fodor et al., 1999), resulting in horizontal extension, often bi-directional (Mandl, 2000). This occurrence is of interest because rock masses cut by normal fault sets, particularly in areas being subjected to extensional deformation, in favourable conditions can act as highly permeable zones for hydrothermal deposits (e.g. Fyfe et al., 1978; Sibson, 1996).

Such conjugate normal fault sets and extension fractures were investigated in an area with well documented stratigraphy—in the southern part of the Holy Cross Mountains (HCM) in Poland (Figs. 1 and 2). In this region, these types of faults and fractures occur commonly side-by-side in Devonian strata. This study examines the evolution of the uplifted rock masses subjected to progressive extension interrupted by longer periods of sedimentation and lithification of deposits.

2. Geological setting

The HCM are located within the Tornquist–Teisseyre Zone forming part of the Trans-European Suture Zone (Berthelsen, 1993) (Fig. 1a). The HCM consist of a Palaeozoic core and a Permo-Mesozoic cover (Figs. 1b and 2). The Palaeozoic core comprises the Łysogóry (northern) and Kielce (southern) tectono-stratigraphic units (Czarnocki, 1919, 1957; Pożaryski, 1978; Stupnicka, 1992). These units are separated by the Holy Cross Fault (Fig. 1b), representing a deep-seated crustal discontinuity (e.g. Kutek, 2001).

* Tel.: +48-22-5540432; fax: +48-22-5540001.
E-mail address: andrzej.konon@uw.edu.pl (A. Konon).

0191-8141/$ - see front matter © 2003 Elsevier Ltd. All rights reserved.
doi:10.1016/j.jsg.2003.08.004

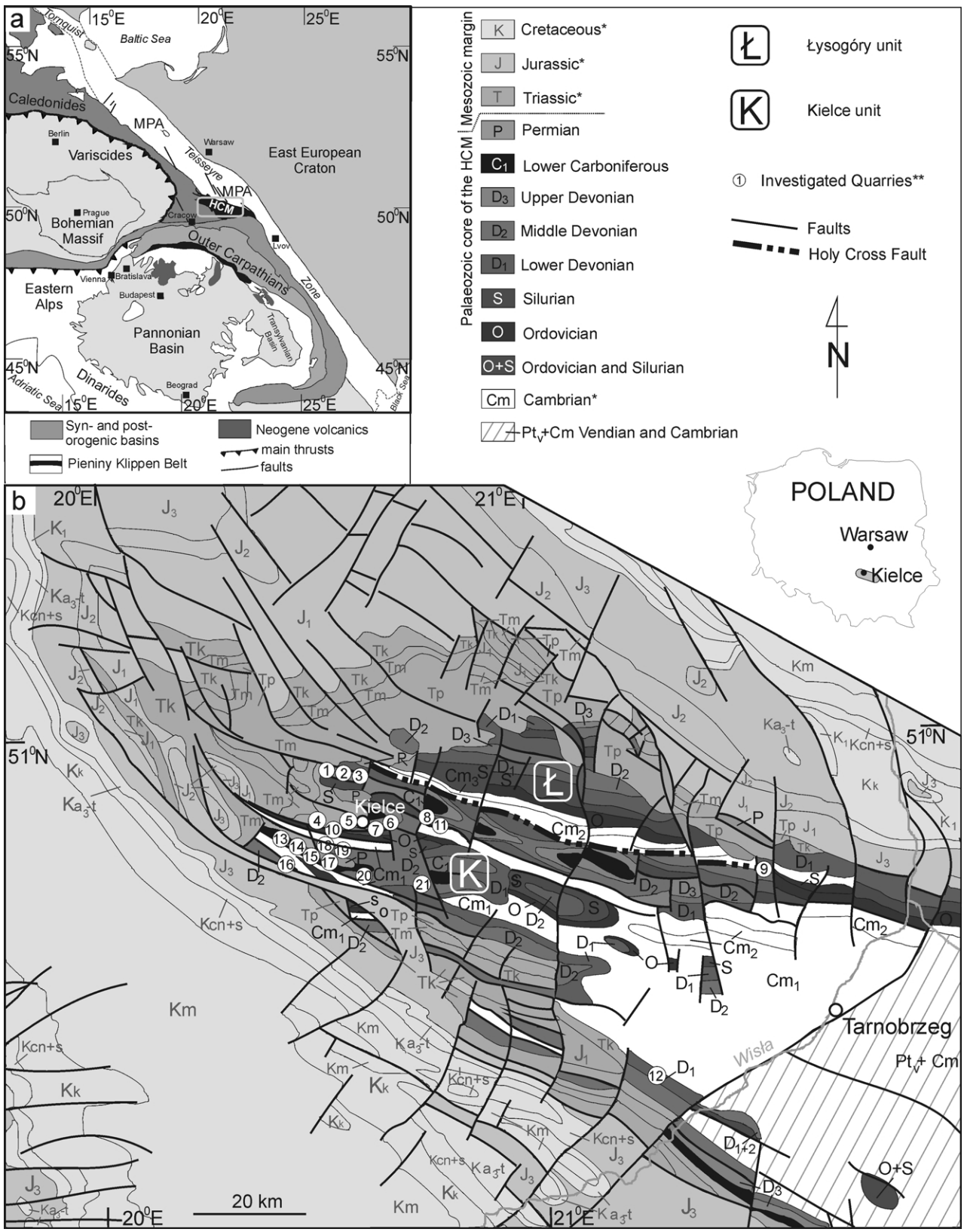

Fig. 1. (a) Tectonic sketch-map of Central Europe (simplified after Guterch et al., 2000). MPA—Mid-Polish Anticlinorium, HCM—Holy Cross Mountains. (b) Geological map of the HCM (after Dadlez et al., 2000). Cambrian*—(Cm_1—Lower; Cm_2—Middle; Cm_3—Upper), Triassic*—(Tp—Buntsandstein; Tm—Muschelkalk; Tk—Keuper), Cretaceous*—(K_1—Lower; Ka_3-t—Upper Albian–Turonian; Kc + t—Cenomanian and Turonian; Ka_3 + c—Upper Albian and Cenomanian; Kcn + s—Coniacian and Santonian; Kk—Campanian; Km—Maastrichtian). Investigated Quarries** : 1. Laskowa; 2. Kostomłoty; 3. Mogiłki; 4. Szczukowskie Górki; 5. Grabina; 6. Wietrznia; 7. Kadzielnia; 8. Górno; 9. Karwów; 10. Jaworznia; 11. Józefka; 12. Jurkowice; 13. Ołowianka; 14. Ostrówka; 15. Zelejowa; 16. Rzepka; 17. Jaźwica; 18. Sitkówka–Kowala; 19. Trzuskawica; 20. Radkowice; 21. Łabedziów. For other explanations see text.

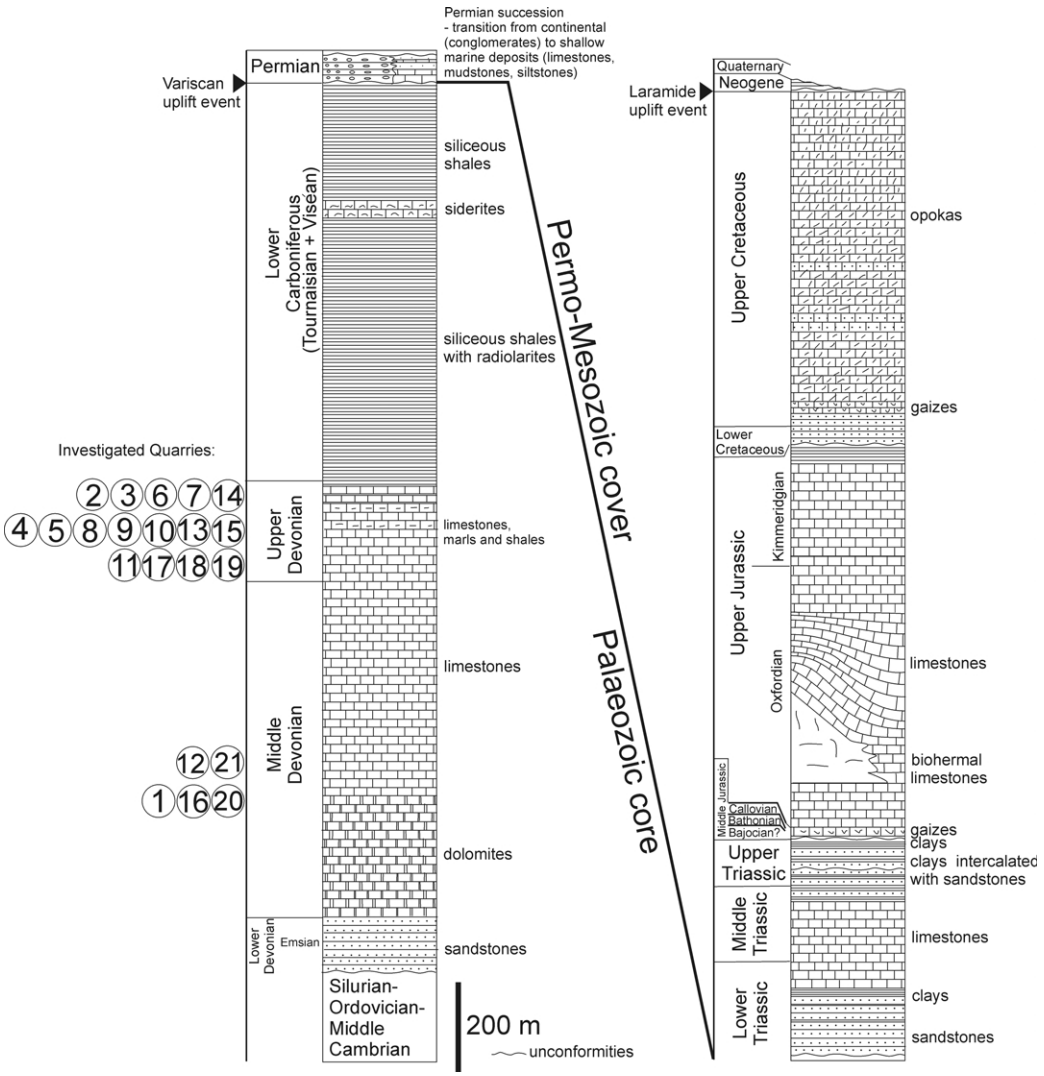

Fig. 2. Lithostratigraphic columns of strata occurring in the Palaeozoic core and Permo-Mesozoic cover of the Kielce unit (based on Hakenberg et al. (1976) and Stupnicka (1992) and references therein). For other explanations see Fig. 1 and text.

Investigations were carried out in Middle and Upper Devonian carbonate rocks of the Kielce unit. Most of these rocks represent the Devonian carbonate platform of the Kielce unit, which existed on the shelf of Laurussia, founded on an Early Palaeozoic basement deformed during Caledonian movements (Szulczewski et al., 1996). The thickness of the Devonian strata is estimated to be between 700 m (Belka, 1990) and 1000 m (Stupnicka, 1992) (Fig. 2). Devonian carbonate rocks are overlain by Lower Carboniferous siliceous shales (Fig. 2). The present thickness of the Tournaisian and Viséan strata in the Kielce unit is estimated as being from 25 m in the Ostrówka quarry (Szulczewski et al., 1996), through about 250 m somewhat farther northwards (Żakowa and Migaszewski, 1995), reaching its maximum in the central parts of the Kielce unit, where a thickness of up to 1000 m has been reported (Żakowa, 1981; Narkiewicz, 1990; Stupnicka, 1992; Żakowa and Migaszewski, 1995) (Fig. 2). During the Late Carboniferous, rocks of the Kielce unit were folded as a result of Variscan deformations (Czarnocki, 1919).

In the Kielce unit, 100–120°-trending regional parallel folds, comprising Lower Cambrian–Lower Carboniferous rocks (Czarnocki, 1938; Stupnicka, 1992) are exposed in a broad belt up to 160 km long and 15–25 km wide (Fig. 1b). The folds are mostly open, concentric and upright without distinct vergences. Rarely, the folds have opposite north and south vergences, when incompetent strata, mainly shales and thin-bedded sandstones, occur in the hinges (Kowalczewski, 1971; Lamarche et al., 1999). Generally, limbs of folds dip approximately 40° to the south and north (Czarnocki, 1938; Stupnicka, 1992). Only in the vicinity of regional faults do these fold limbs dip at up to 85° (Kowalczewski, 1971; Kowalski, 1975).

Due to the uplift that began after the Viséan, a significant thickness of Devonian and Carboniferous rocks was removed by erosion (e.g. Kowalczewski, 1971; Stupnicka,

1992; Belka, 2000). In extreme cases, Cambrian rocks are overlain by Upper Permian rocks and Devonian rocks are covered by Lower Triassic rocks, suggesting that as much as 1 km of deposits were removed in the course of erosion (Czarnocki, 1938; Filonowicz, 1967) (Figs. 1 and 2).

During the Permian and Mesozoic, the area of the HCM was part of the Polish Permo–Mesozoic Rift Basin (Kutek, 2001). As a consequence of the Laramide inversion of the Rift Basin, the Mid-Polish Anticlinorium was formed (Kutek, 2001) (Fig. 1a).

In the HCM, which constitutes part of the Mid-Polish Anticlinorium, this led to further significant deformations that, among other things, resulted in the increase of dips of Variscan fold limbs (e.g. Kowalczewski, 1971; Kutek and Głazek, 1972). The uplift associated with Laramide inversion locally led to the removal of up to 2–3 km of Mesozoic sediments and finally to the exposure of the Palaeozoic core of the HCM (Kutek and Głazek, 1972; Kutek, 2001).

The investigations were carried out in 21 quarries, where Middle and Upper Devonian dolomites and limestones are (or were) exploited (Figs. 1b and 2). The quarries are from 12 to 60 m deep and from 100 m to 2.5 km long. Conjugate normal fault sets with different dihedral angles and sub-vertical fractures with similar strikes were identified on each exploitation level of these quarries. Their regional distribution, cross-cutting relationships and relation to the Mesozoic overburden were noted. Choosing the same stratigraphic level allowed control of the approximated thickness of overburden of the Devonian rocks. This constrain meant that it was possible to estimate the maximum depths to which conjugate normal faults and extension fractures could occur. Based on this analysis, the reconstruction of the tectonic evolution of these structures in the Kielce unit, subjected to strong uplift at least two times, was proposed.

3. Normal faults and fractures

3.1. Mesh-fracture structures

Low-displacement fracture networks occur commonly in Devonian carbonate rocks of the Kielce unit (Fig. 3). These minor calcite-filled fractures are linked and form orderly rhomb-like mesh-fracture structures (Sibson, 1996). The mesh-fracture structures comprise two opposite-dipping sets with strikes ranging from 15 to 30°. The WNW- and ESE-dipping sets form a system that encloses dihedral angles ranging from 40 to 60° (Fig. 3). Both sets are commonly linked with arch-like connections, suggesting simultaneous passing of one set into another, which facilitated the identification of the conjugate shear fracture systems (Jaroszewski, 1972; Mastella and Konon, 2002).

The sense of movement identified mainly due to the occurrence of dilatational jogs points to the fact that, despite

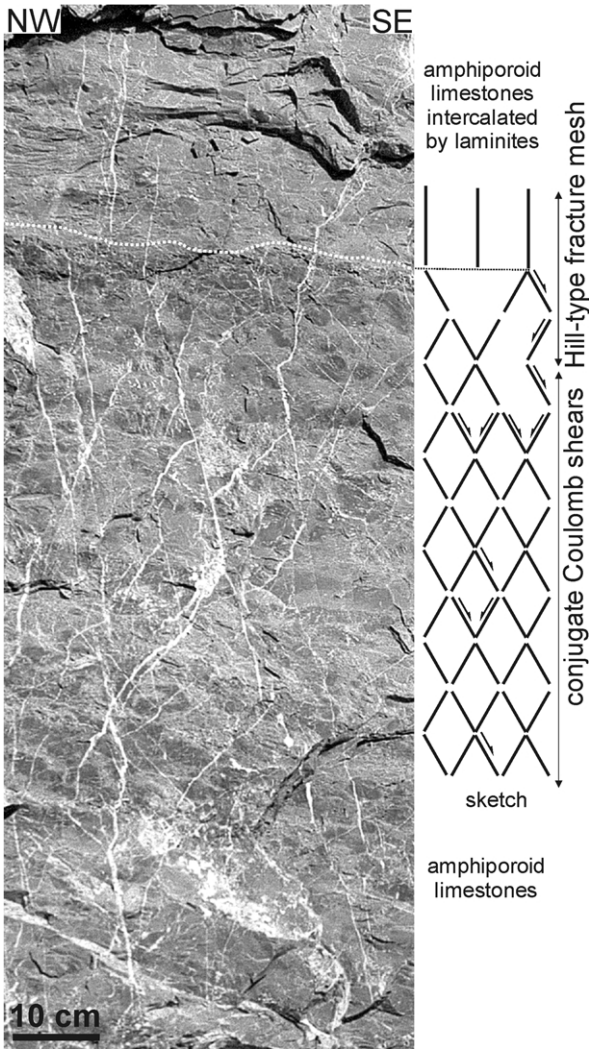

Fig. 3. Mesh-fracture structures on the northern wall of the Ostrówka Quarry (no. 14). For location of the quarry see Fig. 1.

the multi-stage character, normal slip prevailed along these sets. Mesh-fractures, being typical conjugate Coulomb shears, predominate in the Kielce unit. Moreover, locally in beds with strongly variable competency, sub-vertical extension fractures developed within competent layers and conjugate shears developed within incompetent layers, together forming Hill-type fracture meshes (sensu Sibson, 1996) (Fig. 3).

3.2. Normal fault sets

Apart from the mesh-fracture structure, the most common extensional structures in the study area are a series of penetrative dip-slip faults, which post-date the Variscan folding (e.g. Fig. 4a, c and d). Normal faults form two systems: N_P-with strikes perpendicular to the regional fold axes and N_L-with strikes parallel to these axes. Both systems comprise two opposite-dipping fault sets with acute dihedral angles ranging from 11 to 65°. The fault sets of the N_P system are concentrated mainly into two sub-groups:

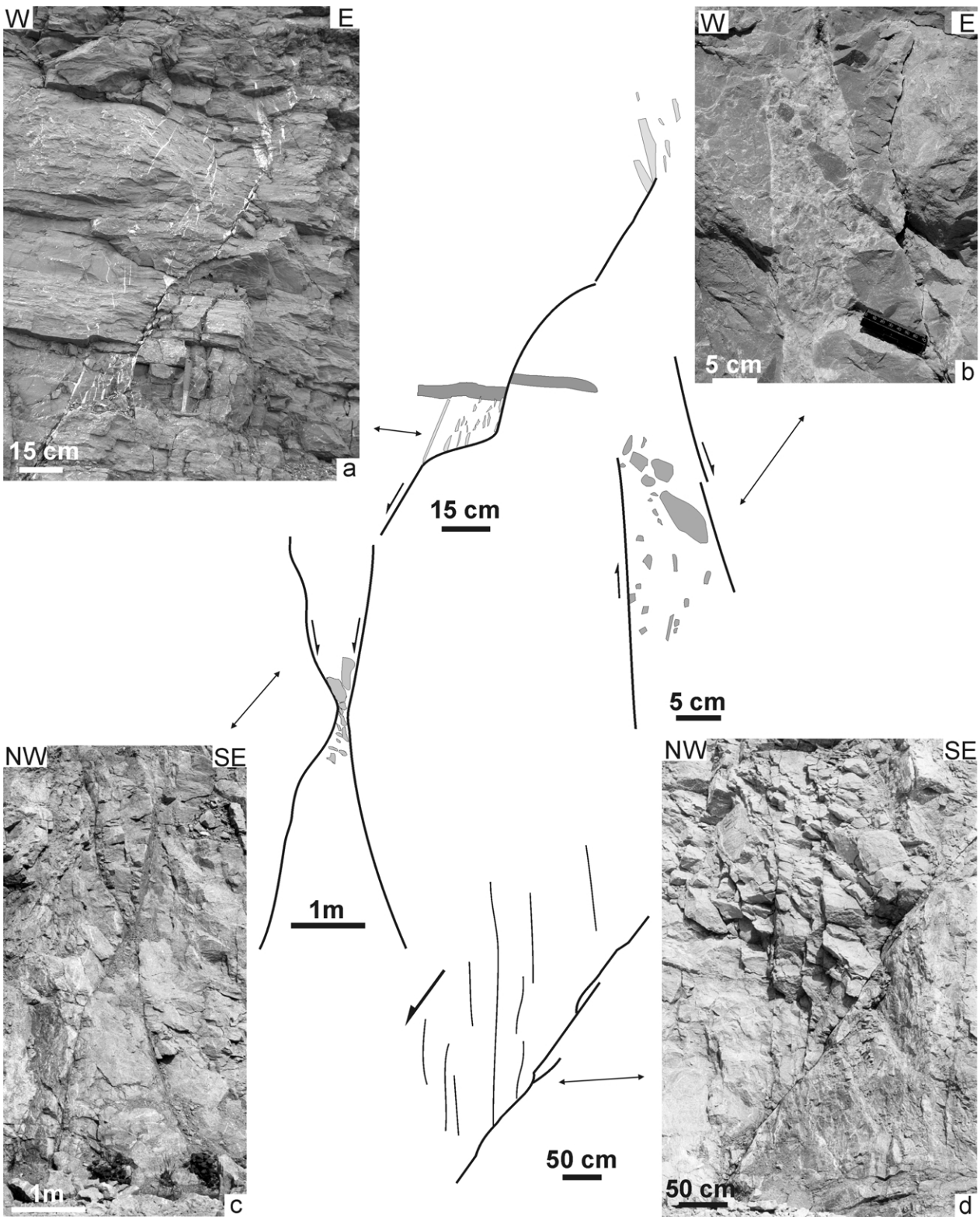

Fig. 4. Examples of different indicators of normal slip along fault planes and connections of the sets. (a) Refraction of fault due to different strengths of thin-bedded limestones and medium-bedded limestones. See the offset of the thin-bedded limestones. Example from the Kostomłoty quarry (no. 2). (b) Dilatational jog from the Trzuskawica Quarry (no. 19). (c) Arch-like connection between two conjugate normal fault sets in the Ostrówka Quarry (no. 14). (d) Horsetail splays of fractures in the hanging wall of the normal fault in the Ostrówka Quarry (no. 14). On drawings, the breccia is marked by a more intensive grey colour and the vein minerals by a lighter grey colour. For location of quarries see Fig. 1.

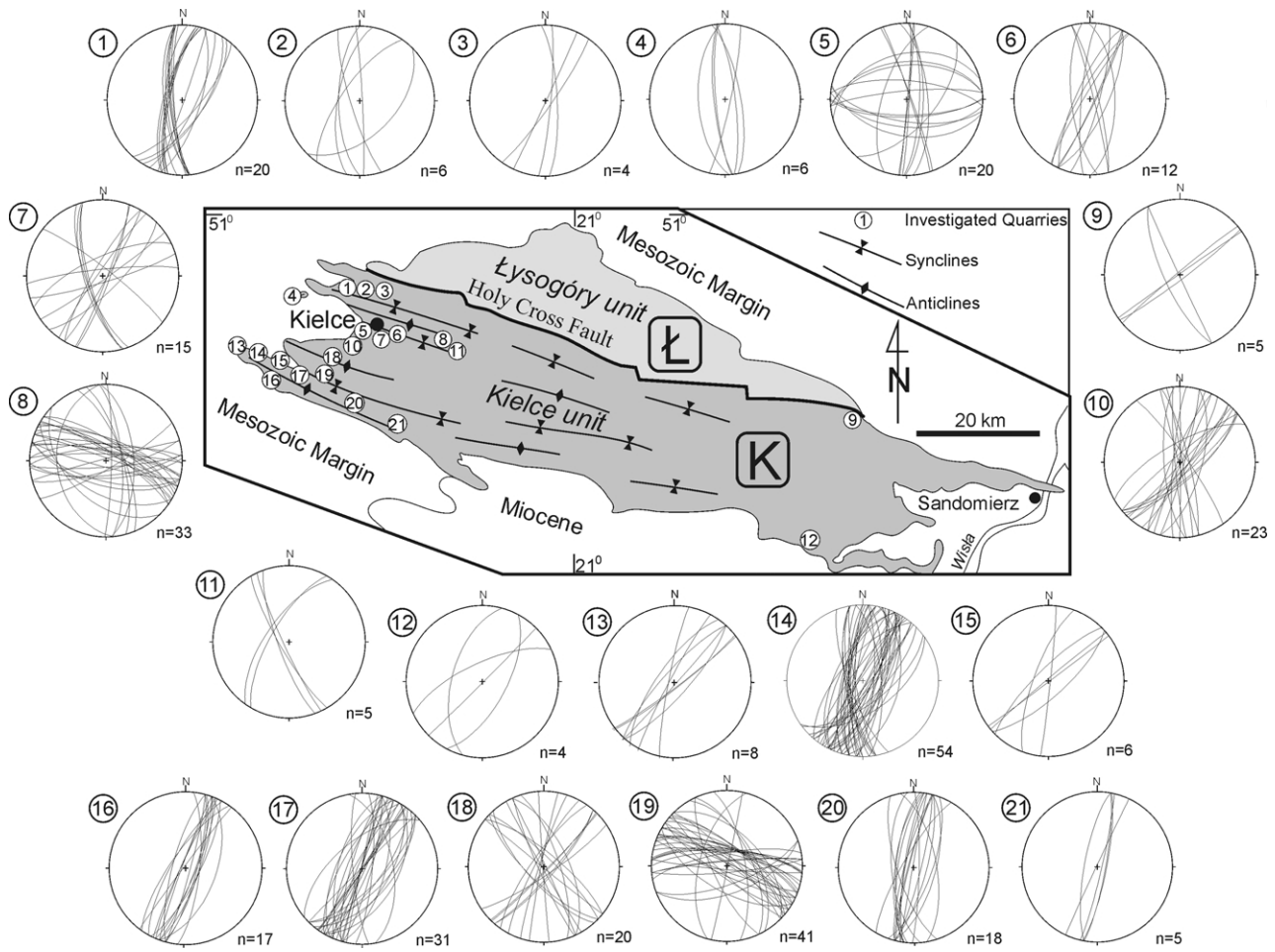

Fig. 5. Lower-hemisphere projections of normal fault and sub-vertical fracture planes (great circles) observed in the Devonian strata of the Kielce unit. Location of quarries presented in Fig. 1b.

WNW-dipping faults with dip directions ranging from 260 to 300° dipping at 50–85° and ESE-dipping faults with dip directions within the interval 90–140° dipping at 50–85° (Fig. 5).

Much rarer than the N_P system are the fault sets of the N_L system, corresponding to NNE- and SSW-dipping faults (quarries 5, 7, 8, 18 and 19 in Fig. 5). The NNE-dipping faults with dip directions within the interval 10–45° dip at 50–85°, whereas SSW-dipping faults with dip directions within the interval 180–230° dip at 50–85° (Fig. 5). The sense of slip along fault planes was identified mainly from the offset of bedding, mineral veins, occurrence of striae, dilatational and compressional jogs (Figs. 4b and 6b and c), as well as horsetail splays of fractures (Fig. 4d). According to these indicators, normal slip predominated in the incipient phase. The presence of younger horizontal striae indicates that some of these faults were reactivated later as strike-slip faults. The fault zones are filled mainly with breccias and gouges (Fig. 4b). The fault breccias are composed of angular, carbonate clasts, up to 10 cm in size. These normal faults have displacements reaching from 0.2 to approximately 2 m. Lengths of fault traces, analysed from photographs of the walls of the quarries, range from 3 to dozens of metres (Figs. 6, 7 and 8c). Similarly, as in the case of mesh-fracture structures, the normal fault sets are also commonly linked with arch-like connections (Fig. 4c). In many cases these faults form a linked rhomb-like network of faults corresponding to fault/fracture mesh-structures (Sibson, 1996, 2000) (Figs. 6c and d and 7).

Conjugate systems of normal faults with different dihedral angles commonly co-occur side by side with sub-vertical fractures in quarries in the same stratigraphic levels.

Fig. 6. (a) Sub-vertical fractures and normal faults occurring side by side in Middle Devonian dolomites on the northern wall of the Rzepka Quarry (no. 16). (b) Calcite-filled sub-vertical fracture F_P (3) cut by younger barren normal fault N_P (2^n). (c) Calcite-filled sub-vertical fracture F_P (3) cut by younger linked rhomb-like network of normal barren faults N_P (2^n). (d) Group of normal faults forming wide mesh-like faults structure. bd—borehole drill. F_P (sub-vertical fractures) and N_P (normal faults) with strikes perpendicular to the regional fold axes. 3- and 2^n-numbers related to relationships between F_P and N_P discussed further in the text. For location of quarry see Fig. 1. For other explanations see text.

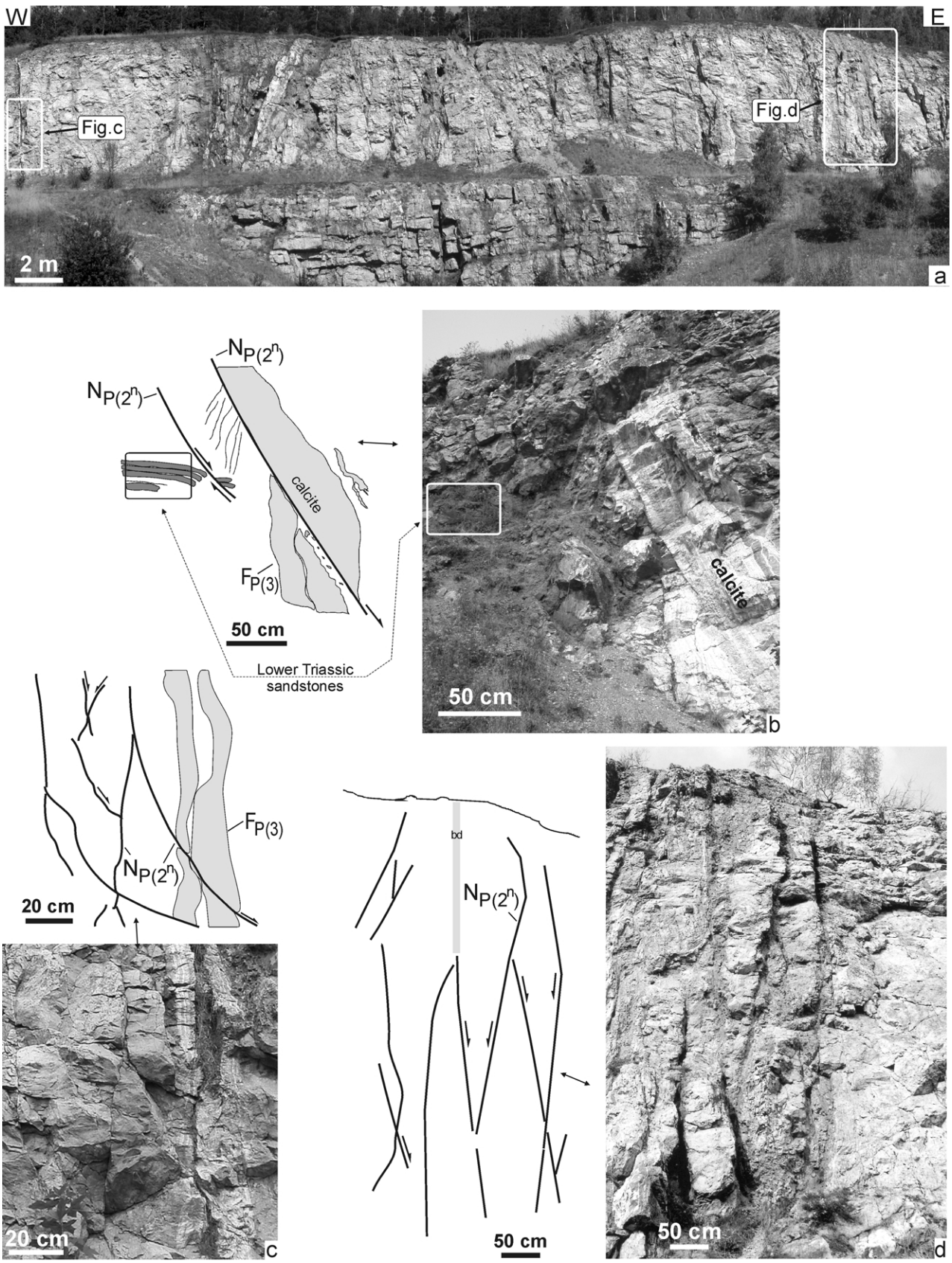
W
E
Fig.c
Fig.d
2 m
a
$N_{P(2^n)}$
$N_{P(2^n)}$
calcite
$F_{P(3)}$
50 cm
Lower Triassic
sandstones
calcite
50 cm
b
$F_{P(3)}$
$N_{P(2^n)}$
20 cm
20 cm
c
bd
$N_{P(2^n)}$
50 cm
50 cm
d

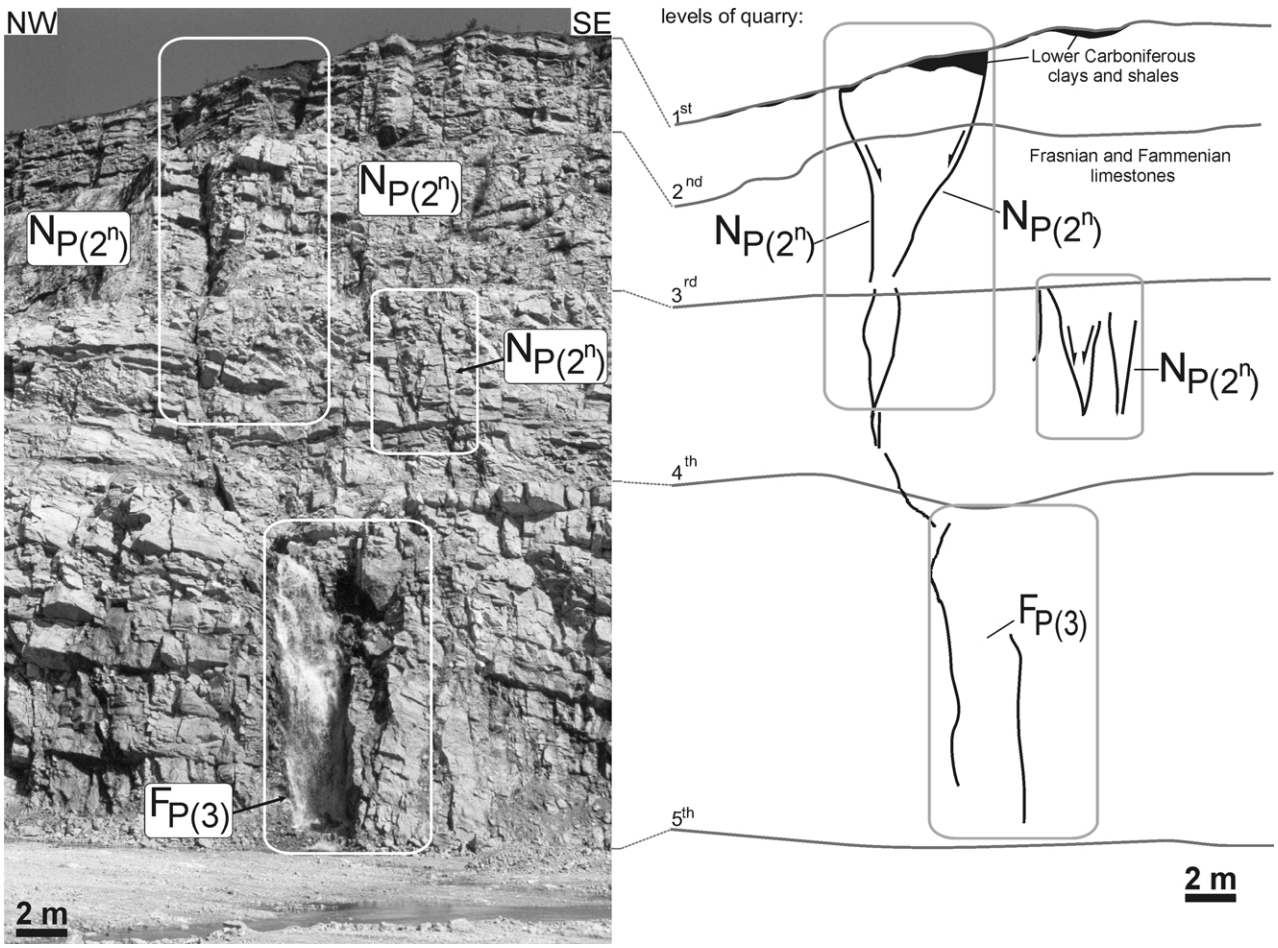

Fig. 7. Normal faults N_P (2^n) and sub-vertical fractures F_P (3) on the northern wall of the Ostrówka Quarry (no. 14). 3- and 2^n-numbers related to relationships between F_P and N_P discussed further in the text. For location of quarry see Fig. 1. For other explanations see text.

Due to this fact it is necessary to distinguish the individual sub-groups of these structures. Based on ranges of the acute dihedral angle (2Θ) values, following the sub-divisions of Hancock (1985) and Dunne and Hancock (1994), faults with $2\Theta > 45°$ and with 2Θ ranging from 11 to 45°, as well as sub-vertical fractures were noted.

3.2.1. Normal faults with $2\Theta > 45°$

Two opposite-dipping normal fault sets enclosing the dihedral acute angle ranging from 45 to approximately 60° were observed relatively rarely in Devonian rocks. Among faults with $2\Theta > 45°$ only the N_P system (WNW- and ESE-dipping faults) was noted. Smooth, planar fault surfaces bounding fault zones prevail; however, slightly curvilinear surfaces also occur (e.g. Fig. 6c). The fault zones of this sub-group, commonly without mineralization, are rather narrow and vary from 5 to about 20 cm in width. In this sub-group, lengths of fault traces, observed on the vertical walls of the quarries, are shortest of all sub-groups of normal fault sets.

3.2.2. Normal faults with $2\Theta = 11–45°$

Normal fault sets enclosing smaller dihedral acute angles (2Θ) ranging from 11 to 45° occur more frequently than the shallow-dipping fault system. Apart from N_P sets, N_L sets were also noted (e.g. Figs. 5 and 9b). The fault sets of this group, similar to the shallow-dipping faults have parallel strikes, opposite dips, and sporadically arch-like connections (Fig. 4c). The fault zones of this sub-group are wider and more frequently calcite-filled (Fig. 8c) in comparison with the system of faults with $2\Theta > 45°$. Moreover, lengths of fault traces are somewhat longer than in the case of the shallow-dipping system.

The normal faults, similar to the shallowly-dipping sets, were repeatedly reactivated. Arrays of minor shears occur on the fault planes coated with calcite. The calcite is often strongly folded and imbricated (Fig. 9a). When the fault zones were reactivated, the younger strata infilling the zones were folded due to dragging along fault planes (Fig. 9b).

3.2.3. Sub-vertical fractures F_P and F_L

A series of steeply-inclined (>85°) fractures, F_P and F_L, are the most frequent of all types of fractures occurring in the Kielce unit. Sub-vertical fractures occurring perpendicularly to the fold axes (F_P) have strikes ranging from 0 to 50° (Fig. 5). Perpendicular to them, similar to the normal faults, a sub-group of sub-vertical fractures (F_L) was rarely

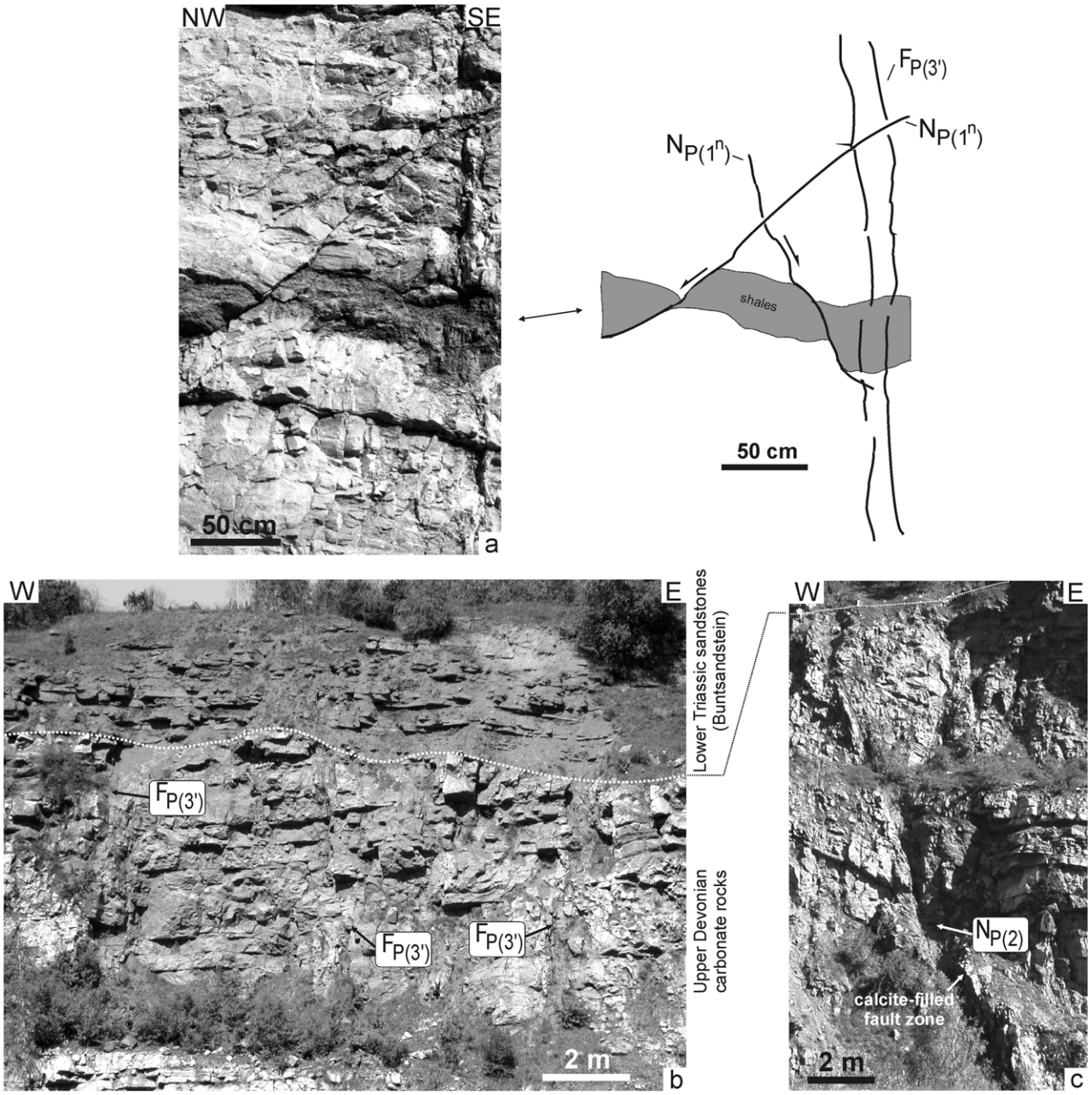

Fig. 8. Examples of the faults and sub-vertical fractures formed during different tectonic events and relations of the sub-vertical fractures to younger strata. (a) Barren sub-vertical fracture F_P ($3'$) cut by younger barren normal fault N_P (2^n) from the Ostrówka Quarry (no. 14). (b) Barren sub-vertical fractures F_P ($3'$) occurring in Frasnian limestones overlain by Lower Triassic strata (Buntsandstein on the northern wall of the Jaworznia Quarry (no. 10). Dashed white line—Variscan unconformity. (c) Calcite-filled normal fault N_P (2) from the Jaworznia Quarry (no. 10). $3'$- and 2-numbers related to relationships between F_P and N_P discussed further in the text. For location of quarries see Fig. 1. For other explanations see text.

noted (Fig. 5). This sub-group has strikes ranging from 110 to 140° (quarries 5, 9, 18 and 19 in Fig. 5).

Most of the sub-vertical fractures extend vertically for at least a few dozen metres (Figs. 6b and c, 7 and 8b). The fracture zones, varying from 0.2 to about 3 m in width, are mostly bounded by rough surfaces (Figs. 7 and 8b). These wide zones are generally filled with calcite (Fig. 6b and c), however, barren fractures (without mineralization) may also occur (Fig. 8a and b). Neither the sub-vertical fractures nor the sub-group of the normal faults with $2\Theta = 11–45°$, with wide calcite-filled zones, cut the Mesozoic rocks. The age of this faults/fractures-filling calcite is associated with pre-Permian (Wrzosek and Wróbel, 1961; Rubinowski, 1971) or with somewhat younger Late Carboniferous/Permian (Lewandowski, 1999, their Fig. 9, cluster 4) and Permian phases of calcite mineralization (Wierzbowski, 1997).

Barren fractures are commonly filled with red clays with muscovite, representing the Lower Triassic–Buntsandstein (Fig. 9b). Their age could be determined due to their relation to the Mesozoic overburden, what can be observed e.g. in

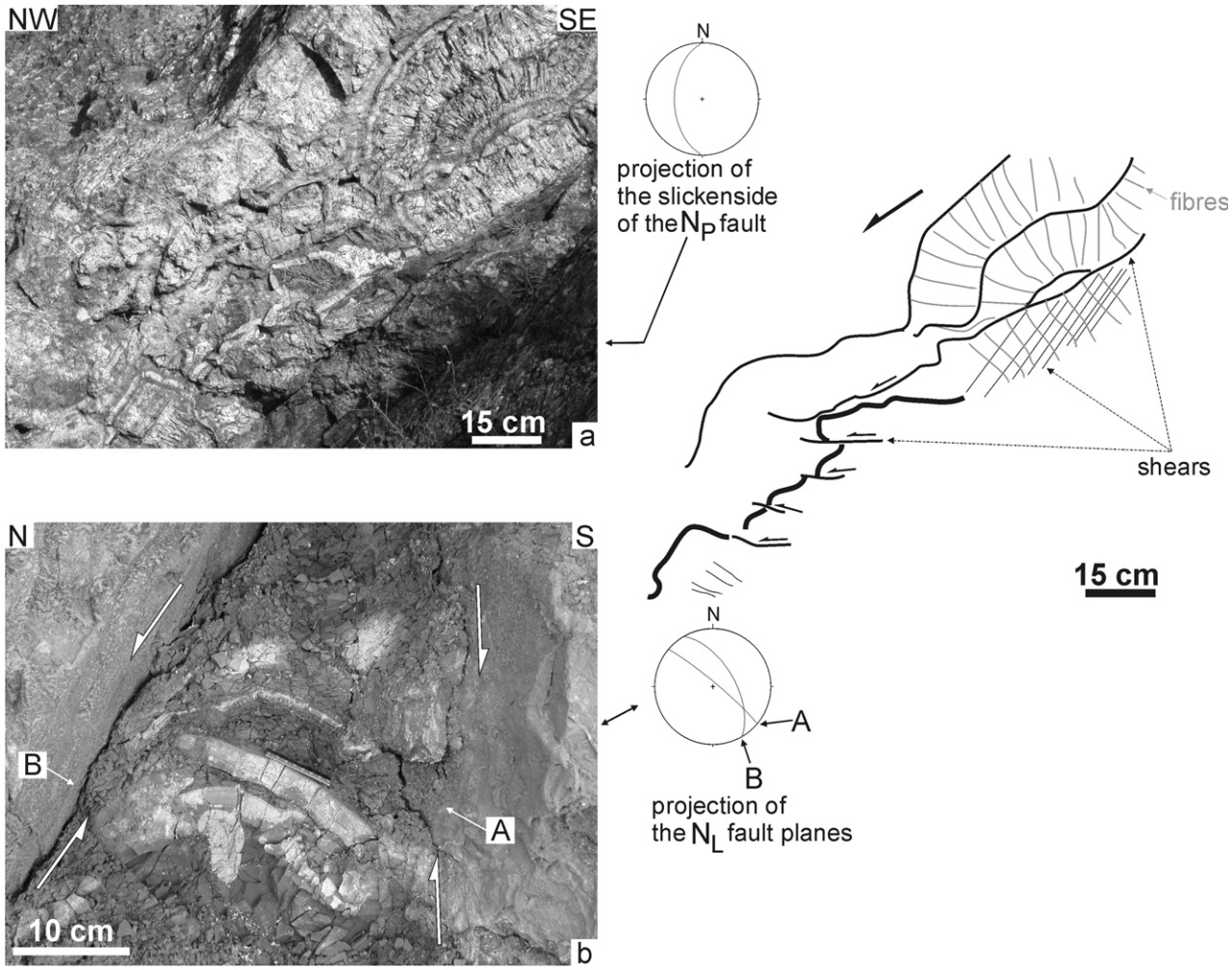

Fig. 9. Examples of fault-related deformations. (a) Folded and imbricated calcite-coated normal fault planes on Zelejowa Mt. (no. 15). (b) Reactivated normal fault zone, filled with Lower Triassic sandstones (Buntsandstein) from the Trzuskawica Quarry (no. 19). For location of quarries see Fig. 1.

quarry no. 10 (Figs. 1 and 5), where Lower Triassic (Buntsandstein) rocks are not cut by these fractures (Fig. 8b).

The sub-vertical fractures and sub-group of the normal faults with $2\Theta = 11–45°$, with wide calcite-filled zones, are commonly cut by barren normal faults. The sub-vertical fractures with wide calcite-filled zones are cut by barren normal faults with $2\Theta = 11–45°$ (e.g. Fig. 6c), which simultaneously offset the Lower Triassic rocks (Fig. 6b). Moreover, the barren sub-vertical fractures are commonly cut by the sub-group of normal faults with $2\Theta > 45°$ (e.g. Fig. 8a). These cross-cutting relationships show that the sub-vertical fractures and normal faults formed during different tectonic episodes.

4. Normal faults and fractures development

Normal faults N_P, N_L, sub-vertical fractures F_P, F_L and mesh fracture structures formed in conditions where the principal stress acted vertically (Fig. 10a), corresponding to the overburden stress (σ_{Vmax}).

Features of the N_P, N_L faults—numerous arch-like connections, parallel strikes and opposite dips point to their coeval formation as conjugate normal fault sets.

Fault sets with acute dihedral angles $2\Theta \geq 45°$ developed in shear conditions when σ_n—the normal stress acting across the fracture—exceeded zero, whereas the least principal stress σ_3 for $2\Theta < 60°$ remained negative (Hancock, 1985; Dunne and Hancock, 1994) (Fig. 10b). Both the normal stress σ_n and the least principal stress σ_3 exceeded zero for $2\Theta \geq 60°$. Similarly, the mesh-fracture structures formed as typical conjugate Coulomb shears (Sibson, 1996).

Steeply-dipping conjugate normal fault sets with values of dihedral angles $2\Theta = 11–44°$ developed in hybrid extension/shear conditions when both the normal stress σ_n and the least principal stress σ_3 were negative (Hancock, 1985; Dunne and Hancock, 1994) (Fig. 10b).

Sub-vertical fractures with wide, often calcite-filled zones, bounded by rough surfaces, without distinct movement indicators developed in extension conditions when the

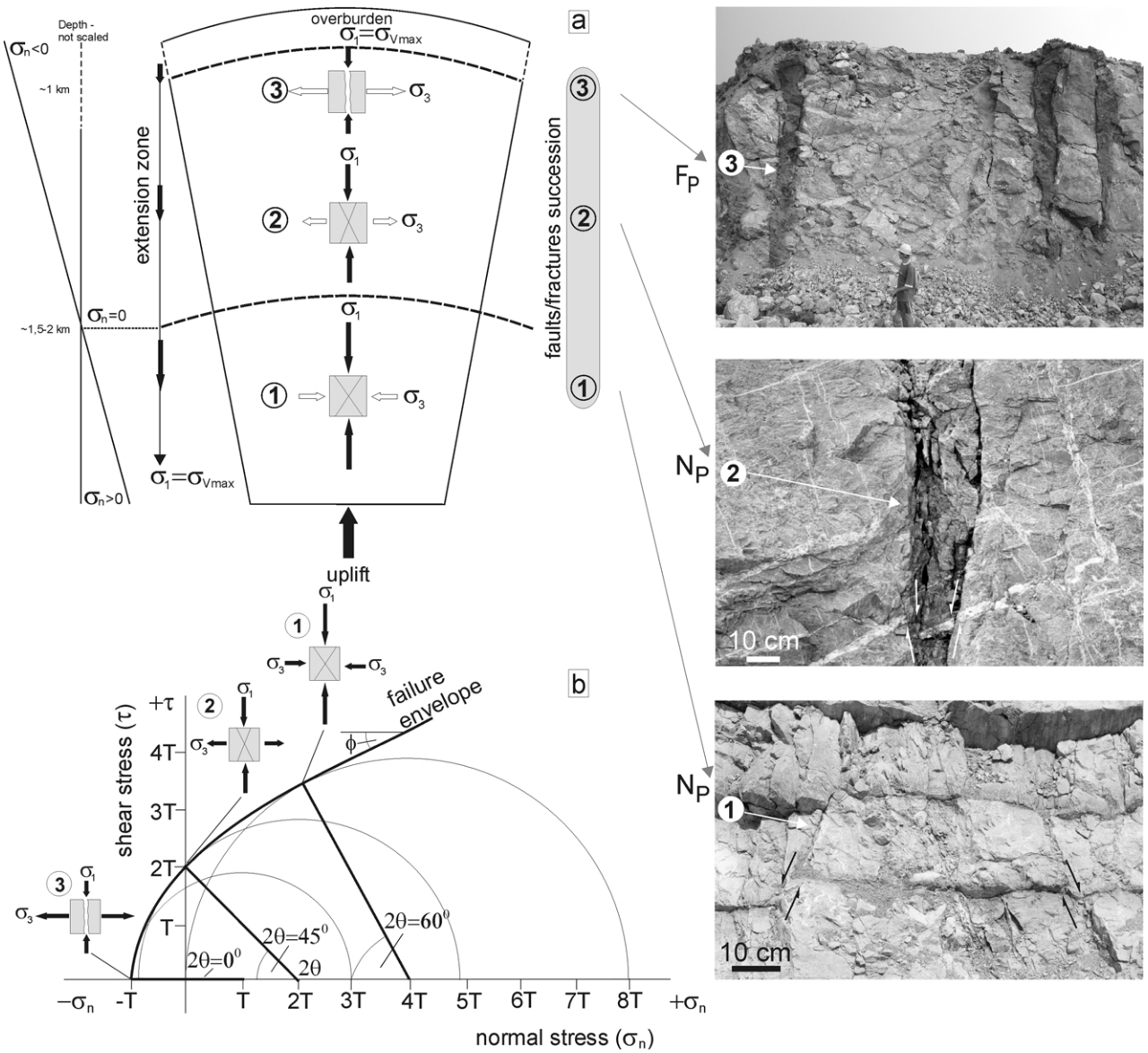

Fig. 10. (a) Simplified model of development of the normal faults/fractures succession. σ_n—normal stress acting across faults and fractures during failure. (b) Composite failure envelope and Mohr circles after Hancock (1985), slightly modified. ϕ—angle of internal friction. For other explanations see text.

normal stress σ_n and the least principal stress σ_3 were negative (Hancock, 1985; Dunne and Hancock, 1994) (Fig. 10b).

The maximum depths to which different types of fracturing can occur form a wide range. For extension fractures, the range of depths at which they can develop is from close to 120 m (Bredehoeft et al., 1976) to, in favourable conditions, even several kilometres (Secor, 1965; Narr and Burruss, 1984; Sibson, 1996).

Estimation of the maximum depth (d_{max}) to which this type of fracturing can occur has been expressed by Secor (1965). According to Secor's formula (1965, no. 11), for the maximum vertical stress axis ($\sigma_1 = \sigma_{Vmax}$):

$$d\max = \frac{3T}{\rho g(1-\lambda)} \quad (1)$$

where T (by Secor noted as K) is the tensile strength of the rock; ρ is the density of the rock; g is the gravitational constant ($g = 981$ cm s^{-2}); λ is the ratio of the pore-fluid pressure relative to the confining pressure, ranging from 0 to 1 (Secor, 1965; Fyfe et al., 1978). Secor also presented a similar equation (Secor, 1965, no. 15) where the greatest and least principal stresses are $8T$ and zero, respectively.

Laboratory obtained data for the Devonian carbonate rocks from the Kielce unit point to densities of rocks (ρ ranging from 2.72 to 2.85 g cm^{-3} and tensile strengths (T) ranging from 5.50 to 7.22 MPa (Pinińska, 1994).

To estimate the maximum depth (d_{max}) it is necessary to know the values of λ. Obtaining the realistic values was possible due to information about the thickness of the overburden of Devonian strata and time of development of the calcite-filled extension fractures. The extension

fractures and normal faults were observed within Middle and Upper Devonian rocks. The extension fractures with wide calcite-filled zones, which cut the folded Devonian strata, are pre-Triassic. The approximated thickness of the Lower Carboniferous rocks, overlying investigated strata, was up to 1 km (Fig. 2). The thickness of the Permian strata did not exceeded 200 m. The total thickness of the Devonian, Lower Carboniferous and Permian strata did not exceeded 2.5 km. It suggests that during the first stage of development of the calcite-filled extension fractures, they could occur at relatively shallow depths up to 1–2 km. According to Secor's formula, for d_{max} ranging from 1 up to 2 km, this group of fractures, both in limestones and dolomites from the Kielce unit, could develop for a low ratio of $\lambda \approx 0.4$—under hydrostatic fluid pressure (Sibson, 1996, 1998, 2000), or for somewhat greater values of λ, but not exceeding a value of 0.7 (Fig. 11).

The maximum depths at which normal faults could occur, based on Secor's equations (1965), were estimated for the increasing values of the effective stress–expressed in T units and for different values of the ratio λ (Fig. 11). For stress conditions favourable for the development of hybrid extensional-shear fractures, the estimated maximum depths are 2.5–3 km if λ reached a value of 0.6 (Fig. 11). Depths at which compressional shear failure appeared are somewhat greater, up to 4–5 km if λ reached values close to 0.6 (Fig. 11).

The mesh-fracture meshes, normal faults and extension fractures are common in the investigated part of the HCM, which suggests that they are penetrative due to strong uplift.

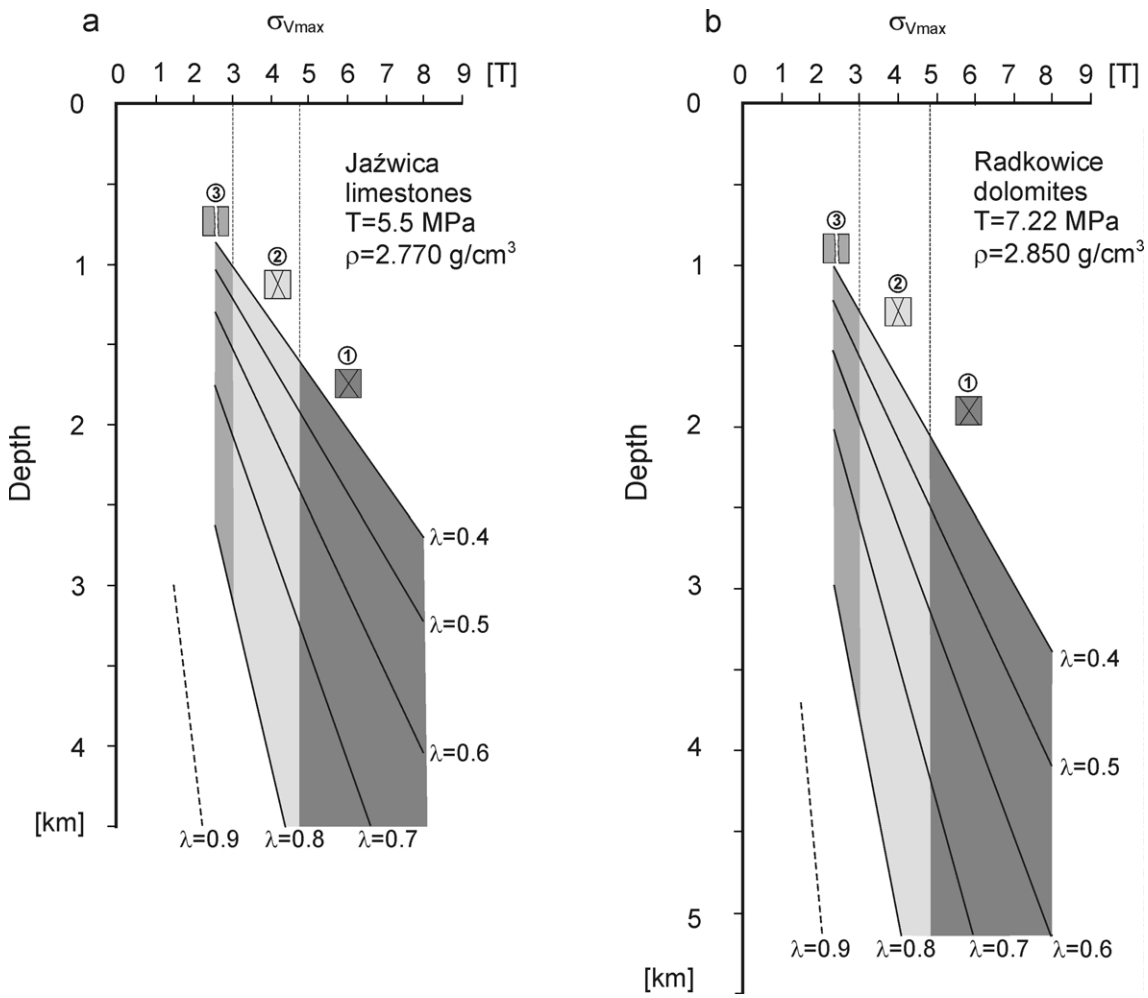

Fig. 11. Graphs showing intervals of depths where different types of normal faults and extension fractures can occur. Graphs are constructed for various magnitudes of σ_{Vmax} with respect to pore fluid pressure, based on Secor's formulas (1965) and composite failure envelope and Mohr circles after Hancock (1985) and Dunne and Hancock (1994). Intervals of σ_{Vmax} for fault/fractures developed in: extension conditions when $\sigma_{Vmax} < 3T$ (—grey), hybrid extension/shear conditions when $3 < \sigma_{Vmax} \leq 4.83T$ (—light grey), shear conditions when $\sigma_{Vmax} > 4.83T$ (—dark grey). (a) Graph for Middle and Upper Devonian limestones in the Jaźwica Quarry (no. 17). (b) Graph for Middle Devonian dolomites in the Radkowice Quarry (no. 20). For location of quarries see Fig. 1b. For other explanations see text.

Although the mesh-fracture structures, conjugate normal fault sets and extension fractures are predicted to develop at different values of differential stress, in the Middle and Upper Devonian carbonate rocks of the Kielce unit they occur within the same stratigraphic level.

At greater depths—close to 2 km—there were favourable conditions for the formation of conjugate normal fault sets with $2\Theta > 45°$ (sub-group 1 in Figs. 10 and 11), gradually towards the top, sets formed with $2\Theta = 11–45°$ (sub-group 2 in Figs. 10 and 11), whereas at relatively shallow depths, ≤ 1 km, conditions typical for the development of extension fractures (sub-group 3 in Figs. 10 and 11) prevailed. This means that these structures developed as an orderly vertical succession (sub-groups 3–2–1) at different depths during gradual evolution, probably during uplifting similar to Price's model of uplift (Price, 1959, 1966). Similarly to Price's model, the upward shifting of the rock masses caused the development of horizontal extension in the upper part of rock masses (Price, 1966) (Fig. 10a).

At greater depths, mesh-fracture structures and conjugate normal fault sets with the dihedral acute angle 2Θ close to 60° developed (sub-group 1 in Fig. 10a). The uplifting of rock masses caused the decrease of the least principal effective stress, resulting in a decrease of the acute dihedral angles between the normal fault sets. During upward shifting, above the faults with $2\Theta \approx 60°$, conjugate normal faults with smaller acute dihedral angles (sub-group 2 in Fig. 10a) and sub-vertical extension fractures (sub-group 3 in Fig. 10a) were formed. When the original thickness of the overburden started being removed, the next faults/fractures succession with 2Θ from 60° up to nearly 0° (sub-groups $3'–2'–1'$ in Fig. 12) started to develop, although slightly below the first succession (sub-groups 3–2–1 in Fig. 12). This resulted in the superimposition of the newly-formed succession on the previously developed faults/fractures (Fig. 12). This process was interrupted when uplift ceased, and was followed by longer periods of sedimentation and lithification.

The repeated occurrence of the uplifting movements caused the development of the next sets of extension fractures and normal faults (sub-groups $3^n–2^n–1^n$ in Fig. 12). Such permanent uplift of rock masses resulted in the side-by-side co-occurrence in quarries of extension fractures and conjugate normal faults with similar strikes and with values of 2Θ angles characteristic of different stress conditions pointing to their development at different depths.

The newly-formed faults had the tendency to develop along existing discontinuities occurring in the folded Devonian rocks and to rejuvenate the older faults and fractures.

The co-occurrence of two sub-groups of normal fault sets (WNW- and ESE-dipping faults) and two much rarer sub-groups (NNE- and SSW-dipping faults), suggests that these fault sets could develop as a result of bi-directional horizontal extension (Mandl, 2000), which is common in the central portions of periclines (Price and Cosgrove, 1990). Similarly, according to Price's model (1966) of extension fractures development during uplifting, the steeply-inclined fracture sets, occurring sub-perpendicularly to each other, could form due to the change of magnitude of the least and intermediate horizontal stresses. However, it is difficult to decide whether the normal faults were strictly simultaneously active, similarly to Reches' model (Reches, 1983; Reches and Dieterich, 1983).

Several phases of uplift can be distinguished in the HCM. The first phase, which resulted in the development of such faults/fractures in Devonian rocks, but not cutting the Lower Triassic strata, occurred during a late phase of the Variscan deformations (Fig. 12).

Successive stages of development of normal faults and extension fractures coincide with subsequent episodes of uplift (Fig. 12). The most significant movements are connected with the Laramide inversion of the Polish Permo–Mesozoic Rift Basin (Kutek and Głazek, 1972; Kutek, 2001), when at least 2–3 km of strata were removed. The greater thickness of the Mesozoic overburden could result in the formation of the next group of faults and fractures above the previously developed one in Devonian rocks (Fig. 12). This led to the co-occurrence of older calcite-filled extension fractures as well as barren conjugate normal fault sets (e.g. Fig. 6b and c). Therefore the values of λ controlled by the thickness of the overburden of Devonian rocks, both in this episode of faults/fractures development and during the older episode, could be similar.

5. Conclusions

The penetrative mesh-fracture structures, extension fractures and conjugate normal fault sets with values of 2Θ angles characteristic of extremely different stress conditions, co-occur in quarries in the southern part of the HCM within Devonian strata. This points to a multiphase development of the faults and fractures, at different depths, associated with various stages of the uplifting of rock masses.

The first event in the development of most of the normal faults and extension fractures present in the Middle–Upper Devonian carbonate rocks is associated with a late phase of Variscan tectonic activity. The successions of conjugate normal faults and extension fractures ($3–2–1$ and $3'–2'–1'$ in Fig. 12) developed at relatively shallow depths, 1–2 km.

Next, the faults/fractures succession ($3^n–2^n–1^n$ in Fig. 12) developed during the most significant later uplifting event resulting from the Laramide inversion of the Polish Permo–Mesozoic Rift Basin, lasting from the Senonian up to the Palaeocene, which caused the formation of the Mid-Polish Anticlinorium (Kutek, 2001). This process finally led to the juxtaposition of the normal faults and extension fractures from different successions.

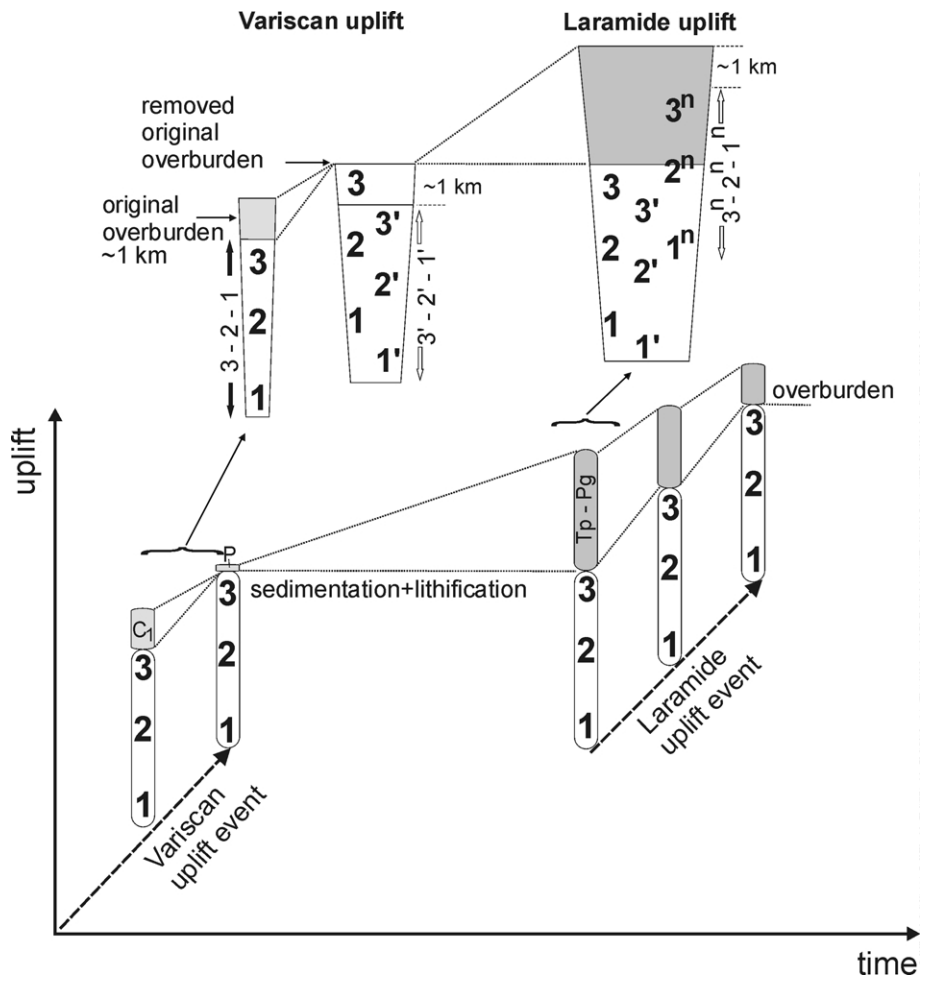

Fig. 12. Sketch showing the hypothetical development of normal faults/fractures successions depending on the proceeding uplift. C_1 (Lower Carboniferous), P (Upper Permian) and Tp–Pg (Lower Triassic–Palaeogene)-strata occurring in the overburden of Devonian strata, respectively, during Variscan, post-Variscan and Laramide uplift events. 3–2–1-initial succession, $3'–2'–1'$-next succession developed below the 3–2–1 succession, $3^n–2^n–1^n$-succession formed above the older successions.

Acknowledgements

I thank Amy Clifton and an anonymous reviewer for their helpful comments and suggestions improving the manuscript; also Leonard Mastella for useful discussions on the origin of the individual structures. I am grateful to Adam Stępień and Michał Śmigielski for their assistance during field work. This paper was supported by grant no. P04D 02621 (Polish State Committee for Scientific Research).

References

Belka, Z., 1990. Thermal maturation and burial history from conodont colour alteration data, Holy Cross Mountains, Poland. Courier Forschung-Institut Senckenberg 118, 241–251.

Belka, Z., 2000. Excursion Guidebook—The Holy Cross Mountains. Joint Meeting of EUROPROBE (TESZ) and PACE Projects. Zakopane/Holy Cross Mountains, Poland, September 16–23, 2000, Warszawa.

Berthelsen, A., 1993. Where different geological philosophies meet: the Trans-European Suture Zone. In: Gee, D.G., Beckolmen, M. (Eds.), EUROPROBE Symposium, Jablonna 1991. Publications of the Institute of Geophysics, Polish Academy of Sciences 255, pp. 19–31.

Bredehoeft, J.D., Wolff, R.G., Keys, W.S., Shuter, E., 1976. Hydraulic fracturing to determine the regional in situ stress field, Piceance Basin, Colorado. Geological Society of American Bulletin 87, 250–258.

Czarnocki, J., 1919. Stratigraphy and tectonics of the Święty Krzyż Mountains. Prace Towarzystwa Naukowego Warszawskiego 28, 1–172.

Czarnocki, J., 1938. Carte géologique générale de la Pologne, feuille 4, Kielce, Edition du Service Géologique de Pologne, scale 1:100,000.

Czarnocki, J., 1957. Tectonics of the Święty Krzyż Mountains. Prace Geologiczne Instytutu Geologicznego 18, 11–138.

Dadlez, R., Marek, S., Pokorski, J., 2000. Geological Map of Poland without Cainozoic deposits. Polish Geological Institute, scale 1:1,000,000.

Doglioni, C., 1995. Geological remarks on the relationships between extension and convergent geodynamic settings. Tectonophysics 252, 253–267.

Dunne, W.M., Hancock, P.L., 1994. Palaeostress analysis of small-scale brittle structures. In: Hancock, P.L., (Ed.), Continental Deformation, Pergamon Press, Oxford, pp. 101–120.

Filonowicz, P., 1967. Detailed Geological Map of Poland, Morawica sheet. Wydawnictwa Geologiczne Warszawa, scale 1:50,000.

Fodor, L., Csontos, L., Bada, G., Györfi, I., Benkovics, L., 1999. Tertiary evolution of the Pannonian Basin system and neighbouring orogens: a

new synthesis of palaeostress data. In: Durand, B., Jolivet, L., Horváth, F., Séranne, M. (Eds.), The Mediterranean Basins: Tertiary Extension Within the Alpine Orogen. Geological Society London Special Publications 156, pp. 295–334.

Fyfe, W.S., Price, N.J., Thompson, A.B. (Eds.), 1978. Fluids in the Earth's Crust. Their Significance in Metamorphic, Tectonic and Chemical Transport. Developments in Geochemistry. Elsevier, Amsterdam, Oxford, New York.

Guterch, A., Grad, M., Keller, G.R., Posgay, K., Vozar, J., Spičak, A., Brueckl, E., Hajnal, Z., Thybo, H., Selvi, O., 2000. The Celebration 2000 Seismic Experiment: abstracts volume. Joint Meeting of EUROPROBE (TESZ) and PACE Projects. Zakopane/Holy Cross Mountains, Poland, September 16–23, 2000, Warszawa.

Hakenberg, M., Kutek, J., Matyja, B., Mizerski, W., Rutkowski, J., Stupnicka, E., Świdrowska, J., Trammer, J., 1976. Stratygrafia, wykształcenie litologiczne i tektonika mezozoiku poludniowo-zachodniego obrzeżenia Gór Świętokrzyskich. In: Pożaryski, W. (Ed.), Przewodnik 47 Zjazdu Polskiego Towarzystwa Geologicznego Starachowice 24–26 września 1976, pp. 185–202.

Hancock, P.L., 1985. Brittle microtectonics: priciples and practice. Journal of Structural Geology 7, 437–457.

Hancock P.L., Bevan T.G., 1987. Brittle modes of foreland extension. In: Coward, M.P., Dewey, J.F., Hanckock, P.L. (Eds), Continental Extensional Tectonics. Geological Society Special Publication 28, pp. 127–137.

Jaroszewski, W., 1972. Mesoscopic structural criteria of tectonics of non-orogenic areas: an example from the north-eastern Mesozoic margin of the Świętokrzyskie Mountains. Studia Geologica Polonica 37, 9–210.

Kowalczewski, Z., 1971. Główne rysy tektoniki Gór Świętokrzyskich. Przewodnik XLIII Zjadu Polskiego Towarzystwa Geologicznego, Kraków. Instytut Geologiczny, Warszawa, pp. 8–19.

Kowalski, W.R., 1975. Tectonics of western end of Checiny anticline and surrounding structures of Mesozoic margins of the Holy Cross Mts. Annales Societatis Geologorum Poloniae 45, 45–61.

Kutek, J., 2001. The Polish Permo–Mesozoic Rift Basin. In: Ziegler, P.A., Cavazza, W., Robertson, A.H.P., Crasquin-Soleau, S. (Eds.), Peri-Tethyan Rift/Wrench Basins and Passive Margins. Peri-Tethys Memoir 6, Mémoires du Muséum National d'Histoire Naturelle 186, pp. 213–236, Paris.

Kutek, J., Głazek, J., 1972. The Holy Cross area, Central Poland, in the Alpine cycle. Acta Geologica Polonica 22, 603–653.

Lamarche, J., Mansy, J.L., Bergerat, F., Averbuch, O., Hakenberg, M., Lewandowski, M., Stupnicka, E., Świdrowska, J., Wajsprych, B., Wieczorek, J., 1999. Variscan tectonics in the Holy Cross Mountains (Poland) and the role of structural inheritance during Alpine tectonics. Tectonophysics 313, 171–186.

Lewandowski, M., 1999. A palaeomagnetic study of fracture fills in the Holy Cross Mountains of Central Poland and its application in dating tectonic processes. Geophysical Journal International 137, 783–792.

Mandl, G. (Ed.), 2000. Faulting in Brittle Rocks: an Introduction to the Mechanics of Tectonic Faults. Springer-Verlag, Berlin, Heidelberg.

Mastella, L., 1988. Structure and evolution of Mszana Dolna Tectonic Window, Outer Carpathians, Poland. Annales Societatis Geologorum Poloniae 58, 53–173.

Mastella, L., Konon, A., 2002. Jointing in the Silesian Nappe (Outer Carpathians, Poland)—paleostress reconstruction. Geologica Carpathica 53, 315–325.

Narkiewicz, M., 1990. Mesogenetic dolomitization in Givetian to Frasnian of the Holy Cross Mountains, Poland. Bulletin of the Polish Academy of Sciences, Earth Sciences 38, 101–110.

Narr, W., Burruss, R.C., 1984. Origin of reservoir fractures in Little Knife Field, North Dakota. American Association of Petroleum Geologists Bulletin 68, 1087–1100.

Pinińska, J. (Ed.), 1994. Właściwości wytrzymalościowe i odkształceniowe skał. Skały osadowe regionu świętokrzyskiego, 1/1. Zakład Geomechaniki IHiGI Wydział Geologii Uniwersytetu Warszawskiego, Warszawa.

Pożaryski, W., 1978. The Świętokrzyski Massif. In: Geology of Poland, 4 Tectonics, Wydawnictwa Geologiczne, pp. 216–227.

Price, N.J., 1959. Mechanics of jointing in rocks. Geological Magazine 96, 149–167.

Price, N.J. (Ed.), 1966. Fault and Joint Development in Brittle and Semi-brittle Rock. Pergamon, Oxford.

Price, N.J., Cosgrove, J.W. (Eds.), 1990. Analysis of Geological Structures. Cambridge University Press, Cambridge.

Reches, Z., 1983. Faulting of rocks in three-dimensional strain fields, II. Theoretical analysis. Tectonophysics 95, 133–156.

Reches, Z., Dieterich, J., 1983. Faulting of rocks in three-dimensional strain fields, I. Failure of rocks in polyaxial, servo-control experiments. Tectonophysics 95, 111–132.

Rubinowski, Z., 1971. The non-ferrous metals ores of the Świętokrzyskie Mountains and their metallogenic position. Biuletyn Instytutu Geologicznego 247, 8–166.

Secor, D.T. Jr, 1965. Role of fluid pressure in jointing. American Journal of Science 263, 633–646.

Sibson, R.H., 1996. Structural permeability of fluid-driven fault-fracture meshes. Journal of Structural Geology 18, 1031–1042.

Sibson, R.H., 1998. Brittle failure mode plots for compressional and extensional tectonic regimes. Journal of Structural Geology 20, 655–660.

Sibson, R.H., 2000. Tectonic controls on maximum sustainable overpressure: fluid redistribution from stress transitions. Journal of Geochemical Exploration 69-70, 471–475.

Stupnicka, E., 1992. The significance of the Variscan orogeny in the Świętokrzyskie Mountains (Mid-Polish Uplands). Geologishe Rundschau 81, 561–570.

Szulczewski, M., Belka, Z., Skompski, S., 1996. The drowning of a carbonate platform: an example from the Devonian–Carboniferous of the southwestern Holy Cross Mountains, Poland. Sedimentary Geology 106, 21–49.

Wierzbowski, H., 1997. Regionalne interpretacje geologiczne na podstawie badań pstrego piaskowca z wypełnień krasowych w okolicach Chęcin (Góry Świętokrzyskie). Przegląd Geologiczny 45, 707–710.

Wrzosek, J., Wróbel, L., 1961. Notes on the occurrence of calcite veins on Zelejowa Mountain near Chęciny. Scientific Bulletins, Academy of Mining and Metallurgy in Cracow, Geology 31, 89–106.

Żakowa, H., 1981. Rozwój i stratygrafia karbonu Gór Świętokrzyskich, Przewodnik LIII Zjazdu Polskiego Towarzystwa Geologicznego, Kielce, pp. 89–100.

Żakowa, H., Migaszewski Z., 1995. The Carboniferous in the Holy Cross Mts. In: Guide to Excursion A2, Development of the Variscan basin and epi-Variscan cover at the margin of the East European platform (Pomerania, Holy Cross Mts., Kraków upland), Polish Geological Institute, pp. 9–11.